Am J Cancer Res 2020;10(12):4178-4197
www.ajcr.us /ISSN:2156-6976/ajcr0121655

Original Article

Oncogene *UBE2I* enhances cellular invasion, migration and proliferation abilities via autophagy-related pathway resulting in poor prognosis in hepatocellular carcinoma

Xiang-Kun Wang[1*], Xi-Wen Liao[1*], Xin Zhou[1], Chuang-Ye Han[1], Zi-Jun Chen[1], Cheng-Kun Yang[1], Jian-Lu Huang[1,2], Jian-Yao Wang[1,3], Jun-Qi Liu[1], Hua-Sheng Huang[1], Shu-Tian Mo[1], Xin-Ping Ye[1], Guang-Zhi Zhu[1], Tao Peng[1]

[1]Department of Hepatobiliary Surgery, The First Affiliated Hospital of Guangxi Medical University, Nanning 530021, Guangxi Province, China; [2]Department of Hepatobiliary Surgery, The Third Affiliated Hospital of Guangxi Medical University, Nanning 530031, Guangxi Province, China; [3]Department of General Surgery, Shenzhen Children's Hospital, Shenzhen 518026, Guangdong Province, China. [*]Co-first authors.

Received September 3, 2020; Accepted November 17, 2020; Epub December 1, 2020; Published December 15, 2020

Abstract: Hepatocellular carcinoma (HCC) is a worldwide malignancy with high morbidity and mortality. In this study, ubiquitin conjugating enzyme E2I (*UBE2I*), a small ubiquitin-like modifier E2 enzyme reportedly expressed in tumors, was examined for its potential effects in HCC. Bioinformatics analysis was performed based on HCCDB, TIMER, and Kaplan-Meier plotter databases to explore the clinical implications in HCC. An siRNA kit was used to downregulate UBE2I, and in vitro experiments-including migration, invasion and proliferation assays-were performed to examine UBE2I expression in HCC. Western blot (WB) was used to determine whether downregulated UBE2I expression influenced the prognosis of HCC via autophagy pathways. Finally, RNA-sequencing was performed to explore candidate molecular mechanisms underlying the effect of UBE2I. Bioinformatics analysis including stratification by alcohol ingestion and hepatitis status in HCC showed that highly expressed UBE2I was not only correlated with poor prognosis, but was also associated with immune infiltrates. In vitro experiments showed that high expression of UBE2I was associated with increased migration, invasion and proliferation of HCC cells. WB results indicated that downregulated expression of UBE2I was associated with higher levels of autophagy-related proteins including LC3A/B, Beclin-1 and ATG16L1. Moreover, RNA-sequencing results suggested that UBE2I was involved in hepatocarcinogenesis, non-alcohol fatty liver disease, steatohepatitis, liver fibrosis, inflammation, hepatoblastoma, tumor angiogenesis, type 2 mellitus diabetes, biliary tract disease and other diseases. We conclude that oncogene *UBE2I* is associated with poor prognosis of HCC via autophagy pathways and may be involved in hepatocarcinogenesis, tumor angiogenesis, non-alcohol fatty liver disease and inflammation.

Keywords: Hepatocellular carcinoma, *UBE2I*, autophagy pathway, prognosis, RNA-sequencing

Introduction

Hepatocellular carcinoma (HCC) is the sixth most common malignant tumor and ranks as the third leading cause of tumor-related deaths worldwide [1]. Due to delays in the early diagnosis of HCC, the disease has resulted in higher mortality worldwide [2, 3]. Although several novel chemotherapeutic drugs have been introduced in clinical applications, surgery remains the most effective treatment for HCC patients [1]. However, surgical resection is limited in treating HCC due to the high incidence of recurrence, as well as intrahepatic and extra-hepatic metastasis [4-6], which means that the long-term survival of HCC patients remains poor. The highly sensitive biomarker alpha-fetoprotein has been used to predict the clinical survival of HCC patients after surgical resection, but the results have been unsatisfactory [7]. Therefore, it is critical to identify novel markers involved in the molecular mechanisms of HCC for early diagnosis and long-term surveillance.

In contrast to other post-translational modifications such as phosphorylation and acetylation, sumoylation adds a small ubiquitin-like modifi-

er (SUMO) polypeptide to the ε-amino group of lysine residues [8-10]. In humans, there are four SUMO proteins, SUMO 1, 2, 3 and 4 [11]. SUMO 2 and 3 are highly homologous to each other and are similar to SUMO 1 [8, 10]. Reminiscent of ubiquitination, sumoylation is catalyzed by a three-enzyme cascade, which is composed of a single heterodimeric E1 activating enzyme, a single E2 conjugating enzyme and multiple E3 ligases [9, 10]. From yeast to humans, ubiquitin conjugating enzyme E2I (UBE2I), previously named ubiquitin conjugating enzyme 9 (UBC9), is the single SUMO E2 enzyme and thus provides a convenient intervention point for globally interrogating how sumoylation modulates many kinds of biological processes in these species [11]. In adipose tissue, UBE2I expression is positively associated with a marker of insulin resistance and corresponds with impaired browning of human white adipocytes, while the UBE2I/microRNA-30a axis regulates mitochondrial activity in human white adipocytes [12]. In lung cancer, Ping et al. demonstrated that upregulated UBE2I promotes cell invasion and metastasis of lung cancer cells, suggesting an important role in cancer progression [13]. In epithelial ovarian cancer, Li et al. showed that UBE2I promotes cell proliferation and therefore plays a pivotal role in this cancer through the PI3K/AKT pathway [14]. In glioma, Shengkui et al. found that UBE2I, also upregulated in glioma tissues, is negatively correlated with the prognosis of patients with glioma, indicating it may be a prognostic indicator of glioma [15]. Given the above research focused on UBE2I in tumors, we explored the potential role of UBE2I in HCC by bioinformatics analysis and functional experiments and identified candidate molecular mechanisms underlying the involvement of UBE2I in HCC progression.

Materials and methods

Analysis of differential expression and prognostic significance

The tumor immune estimation resource (TIMER; https://cistrome.shinyapps.io/timer/) database was used for differential analysis of UBE2I in humans and immune infiltrates in HCC [16, 17]. In addition, the HCCDB (http://lifeome.net/database/hccdb/home.html) database was used to explore the prognostic significance of UBE2I in HCC and related co-expressed proteins [18].

Validation of prognostic significance and construction of a gene-gene interaction network using gene ontology (GO) terms and KEGG pathways of UBE2I-related co-expressed genes

For validation of differential expression and its prognostic significance, Gene Expression Profiling Interactive Analysis (GEPIA, http://gepia2.cancer-pku.cn/#index) [19] and Kaplan-Meier plotter (https://kmplot.com/analysis/index.php?p=service&cancer=liver_rnaseq) [20] databases were employed to examine prognostic significance to perform a stratified analysis by gender and race of UBE2I in HCC. Moreover, a gene-gene interaction network was visualized via geneMANIA plugin of Cytoscape version 3.8.0 [21, 22]. To further explore potential molecular mechanisms underlying UBE2I involvement in HCC, UBE2I and its co-expressed related genes were used to construct an interaction network using the CluGO plugin of Cytoscape version 3.8.0 software [23]. Co-expressed genes were identified from the Cbioportal (https://www.cbioportal.org/) database [24, 25].

Cell culture and cell transfection, RT-PCR and WB assays

To further determine the functions of *UBE2I* in HCC, HCCM and Huh7 cell lines were kindly provided by Prof. Guo-Dong Lu, National university of Singapore and were used for in vitro experiments [26]. Cells were cultured in high sugar Dulbecco's Modified Eagle's Medium (DMEM, Gibco, 8120113) with 10% fetal bovine serum (BI, 1903226), 1% of 100 U/mg penicillin and 100 μg/ml streptomycin (Solarbio, 20191203). Cells were cultured in 5% CO_2 at 37°C. siRNA for UBE2I was purchased from the Ribobio company (siBDM1999A). Antibodies against UBE2I and GAPDH for western blot (WB) were purchased from Abcam (ab75854) and Aksomics (KC-5G5), respectively. Liposome lipo6000 was purchased from Beyotime (C0526).

Cell transfection was performed according to company instructions in five groups as follows: 5 μl of siRNA (1, 2, 3) +5 μl Lipo6000 transfection reagent, negative control (NC, 5 μl NC + 5 μl Lipo6000 transfection reagent), and mock group (5 μl DMEM + 5 μl Lipo6000 transfection reagent). Cells were treated with the siRNA mixtures for 6 h, then washed with sterile PBS and cultured in DMEM with 10% fetal

bovine serum. The cells were extracted 48 h later using TRIzol reagent (Invitrogen, 15596026) to obtain total RNA for RT-PCR, or were lysed in RIPA reagent (Solarbio, R0010) after 72 h to obtain total protein for WB. Relative mRNA expression in the different groups was compared using the $2^{-\Delta\Delta CT}$ method. Primers for *UBE2I* and *GAPDH* were as follows: *UBE2I* Forward: AAAAATCCCGATGGCACGATG, Reverse: CTTCCCACGGAGTCCCTTTC; *GAPDH* Forward: GTCAGCCGCATCTTCTTT, Reverse: CGCCCAATACGACCAAAT. WB assays were performed to determine protein expression in the different groups.

Assays of cell invasion, migration and proliferation ability

Cell invasion ability was determined by Transwell assay. Matrix gels (8.7 mg/ml, 356234) was diluted according to instructions and was added to the upper chamber of Transwell plates (3422, Corning). A total of 1×10^5 cells was resuspended using DMEM and seeded in the upper chamber. The lower chamber received 800 μl medium containing FBS, penicillin and streptomycin. After 24 h, the Transwell chambers were firstly fixed in 800 μl of methanol and then stained in Crystal Violet Stain solution for 30 min. Then, cells were counted under the microscope before comparison.

Cell migration ability was determined using a wound healing assay. Cells were seeded in a six-well plate. Cell monolayers were scratched, and wound healing was assessed by measuring the gap distance at 0, 24 and 48 h. Cell proliferation assays were performed using MTT method (BB-4201, Bestbio). Cells transfected at 48 h were seeded into 96-well plates at 2000 cells/well. Then, cells were treated with 10 μl of MTT solution and incubated for 4 h. The cells were then extracted using 150 μl of MTT dissolving solution and mixed at low speed. Optical density was measured at 550 nm.

Determination of autophagy-related pathways of UBE2I

To further explore whether *UBE2I* utilizes an autophagy pathway, the Autophagy Antibody Sampler Kit (Cell Signaling Technology, #4445), including LC3A/B, ATG3 and Beclin-1 antibodies, was used for WB assay. Antibodies against these proteins were purchased from Cell Signaling Technology and diluted according to instructions. GAPDH was used as an internal control.

Further exploration of molecular mechanisms by RNA-sequencing analysis

We next explored molecular mechanisms by RNA-sequencing analysis using the DESeq2 method in HCCM and Huh7 cells in Novogene company [27]. First, differentially expressed genes (DEGs) were determined using the following criteria: $|\log_2\text{FoldChange}| > 0$, adjusted $P \leq 0.05$. Then, enrichment analysis of GO terms, Kyoto Encyclopedia of Genes and Genomes (KEGG) pathways, Reactome pathways, disease ontology (DO) terms and DisGeNET was performed to further explore candidate molecular mechanisms underlying UBE2I involvement.

Statistical analysis

Graphpad 8.0 was used to construct box plots. Unpaired *t*-test was employed for comparisons for each two groups. Kaplan-Meier plots were constructed for survival analysis. Image J software was used for densitometric analysis. $P \leq 0.05$ was considered statistically significant.

Results

Analysis of differential expression and clinical significance

Analysis of differential expression showed that UBE2I was differentially expressed in several cancers, including HCC, bladder urothelial carcinoma, breast invasive carcinoma, cholangio carcinoma, colon adenocarcinoma, lung adenocarcinoma, rectum adenocarcinoma, kidney renal clear cell carcinoma, and others (all $P < 0.001$, **Figure 1A**). Immune infiltrate analysis indicated that UBE2I expression was positively correlated with B cell, CD8+ T cell, macrophage, neutrophil and dendritic cell infiltration levels (all $P < 0.001$, **Figure 1B**) but not with cell purity or CD4+ T cell infiltration. In addition, the HCCDB database showed that patients with high expression of UBE2I exhibited poor prognosis in HCC (Log-rank $P = 0.011$, **Figure 1C**). Co-expression network analysis indicated that UBE2I was associated with CFL1,

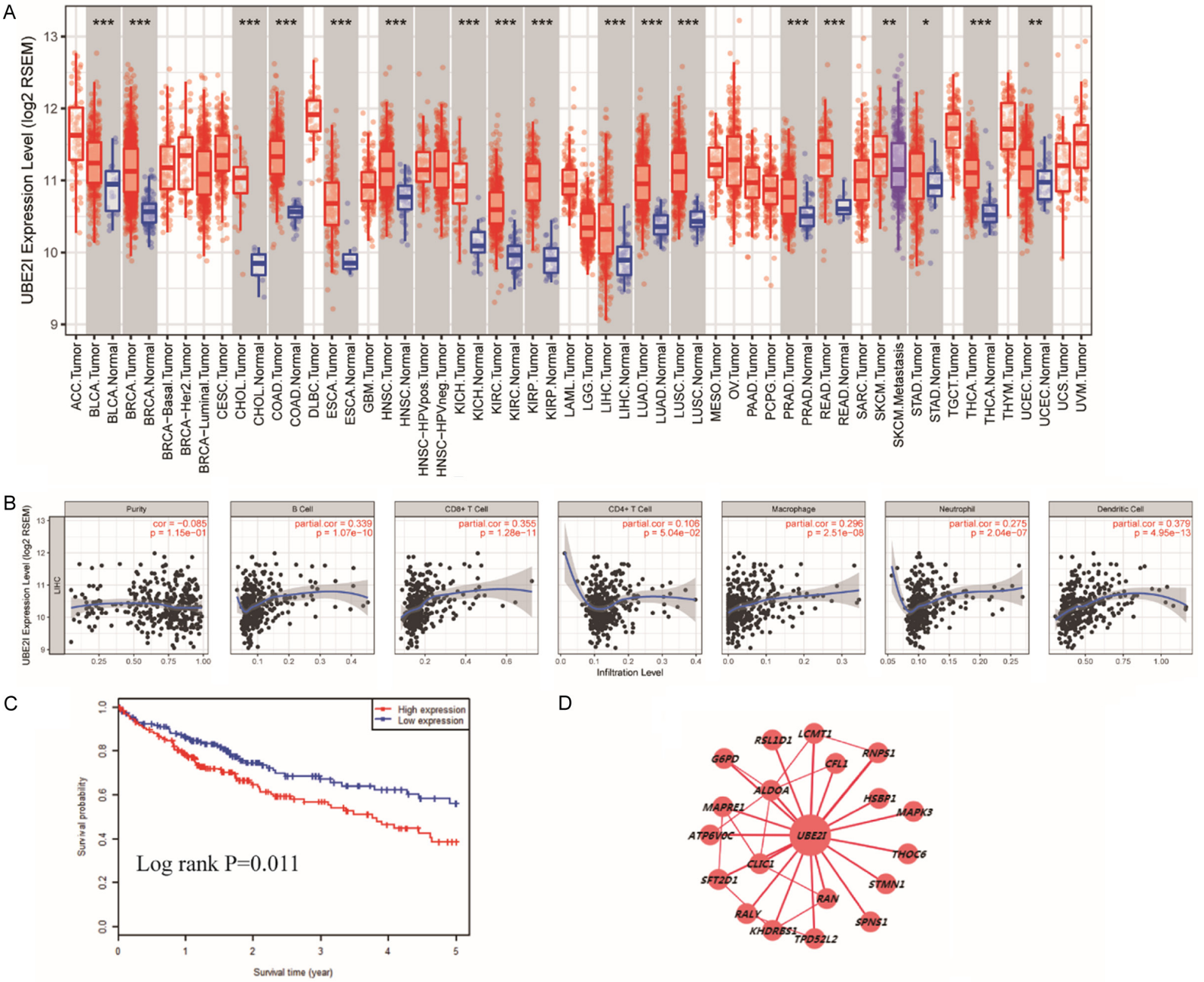
A
UBE2I Expression Level (log2 RSEM)
ACC.Tumor
BLCA.Tumor
BLCA.Normal
BRCA.Tumor
BRCA.Normal
BRCA−Basal.Tumor
BRCA−Her2.Tumor
BRCA−Luminal.Tumor
CESC.Tumor
CHOL.Tumor
CHOL.Normal
COAD.Tumor
COAD.Normal
DLBC.Tumor
ESCA.Tumor
ESCA.Normal
GBM.Tumor
HNSC.Tumor
HNSC.Normal
HNSC−HPVpos.Tumor
HNSC−HPVneg.Tumor
KICH.Tumor
KICH.Normal
KIRC.Tumor
KIRC.Normal
KIRP.Tumor
KIRP.Normal
LAML.Tumor
LGG.Tumor
LIHC.Tumor
LIHC.Normal
LUAD.Tumor
LUAD.Normal
LUSC.Tumor
LUSC.Normal
MESO.Tumor
OV.Tumor
PAAD.Tumor
PCPG.Tumor
PRAD.Tumor
PRAD.Normal
READ.Tumor
READ.Normal
SARC.Tumor
SKCM.Tumor
SKCM.Metastasis
STAD.Tumor
STAD.Normal
TGCT.Tumor
THCA.Tumor
THCA.Normal
THYM.Tumor
UCEC.Tumor
UCEC.Normal
UCS.Tumor
UVM.Tumor
B
Purity
cor = −0.085
p = 1.15e−01
B Cell
partial.cor = 0.339
p = 1.07e−10
CD8+ T Cell
partial.cor = 0.355
p = 1.28e−11
CD4+ T Cell
partial.cor = 0.106
p = 5.04e−02
Macrophage
partial.cor = 0.296
p = 2.51e−08
Neutrophil
partial.cor = 0.275
p = 2.04e−07
Dendritic Cell
partial.cor = 0.379
p = 4.95e−13
LIHC
Infiltration Level
C
High expression
Low expression
Survival probability
Log rank P=0.011
Survival time (year)
D
RSL1D1
LCMT1
G6PD
CFL1
RNPS1
ALDOA
HSBP1
MAPRE1
MAPK3
ATP6V0C
UBE2I
THOC6
CLIC1
SFT2D1
STMN1
RAN
RALY
SPNS1
KHDRBS1
TPD52L2

Figure 1. Clinical analysis of UBE2I in HCC. A: Differential expression analysis of UBE2I in various cancers. B: Analysis of UBE2I expression and immune infiltrates. C: Survival analysis of UBE2I expression in HCC (low = 178, high = 178). D: Co-expression network of UBE2I and co-expression-related genes.

RNPS1, HSBP1, MAPK3, THOC6, STMN1, CLIC1, SFT2D1, G6PD, LCMT1, ALDOA, and others (**Figure 1D**).

Validation of differential expression, prognostic significance and molecular mechanisms of related co-expressed-genes

Differential expression of UBE2I was validated in the GEPIA database, which showed that UBE2I was differentially and highly expressed in HCC compared with non-tumorous tissue ($P < 0.05$, **Figure 2A**). A gene-gene interaction network was constructed which indicated that UBE2I had physical interactions with MITF, RANGAP1, RAD52, ETV6, and other proteins (**Figure 2B**). The prognostic significance of UBE2I was validated by the Kaplan-Meier plotter website, which showed that high expression of UBE2I was associated with poor OS, RFS, PFS, and DSS in HCC (Log-rank $P = 0.016$, 0.013, 0.011 and 0.015, respectively; **Figure 2C-F**). Then, stratified analysis according to HCC risk factors-alcohol consumption and hepatitis infection status-was performed for overall survival (OS), recurrence-free survival (RFS), progression-free survival (PFS) and disease-specific survival (DSS). In an alcohol-drinking population, high expression of UBE2I was associated with poor prognosis only for RFS (Log-rank $P = 0.047$, **Figure 3E**) not others (**Figure 3A**, **3I**, **3M**). However, in a non-drinking population, high expression of UBE2I was associated with poor prognosis for OS, RFS, PFS and DSS (all $P \leq 0.05$, **Figure 3B**, **3F**, **3J**, **3N**). In a hepatitis-infected population, UBE2I expression did not show any significant differences (**Figure 3C**, **3G**, **3K**, **3O**). Nonetheless, high expression of UBE2I was associated with poor prognosis for OS, RFS, PFS and DSS (all $P \leq 0.05$, **Figure 3D**, **3H**, **3L**, **3P**).

The top 100 co-expressed genes related to UBE2I were determined and are shown in Table S1. These results indicated that these genes were involved in protein targeting in peroxisome, glycolysis, positive regulation of ubiquitin-protein transferase activity, protein homotetramerization, regulation of chromosome segregation, regulation of chromatid segregation, central carbon metabolism in cancer, NADP binding and spliceosome snRNP complex, among others (**Figure 4**).

Downregulation of UBE2I expression by siRNA and assays of migration, invasion and proliferation

Downregulating expression of UBE2I was performed using an siRNA kit. Real-time PCR and WB consistently indicated that siRNA 2 (Si 2) was the most effective at suppressing UBE2I expression (**Figure 5A-F**). Therefore, siRNA 2 (Si 2) was used for further experiments.

In invasion assays, downregulating *UBE2I* reduced cell movement through the transwell membrane compared with the NC group for both HCCM and Huh7 cells (both $P < 0.001$, **Figure 6A-F**), which indicated lower invasive capacity resulting from down-regulated expression of *UBE2I*. In migration assays, downregulating *UBE2I* resulted in reduced migration distance compared to the NC group for both HCCM and Huh7 cells at 24 h and 48 h (all $P < 0.001$, **Figure 7A-D**), which indicated lower migratory capacity produced by downregulated *UBE2I* expression. Proliferation assays showed that downregulation of *UBE2I* induced lower OD values compared with the NC group at 0 h, 24 h, 48 h and 72 h (all $P < 0.05$, **Figure 8A**, **8B**), indicating lower proliferative ability with downregulated *UBE2I* expression. However, there was no significant difference between OD values in Huh7 cells at 24 h.

Involvement of autophagy-related pathways in UBE2I expression

To determine if UBE2I expression influences the prognosis of HCC via an autophagy pathway, we tested autophagy pathway-related proteins including LC3A/B, Beclin-1 and AGT16L1. WB results indicated that high expression of UBE2I was accompanied by low expression of LC3A/B, Beclin-1 and AGT16L1 in HCCM and Huh7 cells compared with downregulated UBE2I expression, especially in HCCM cells (all $P < 0.05$, **Figure 8C**, **8D**). However, there was no significant difference between the two groups in terms of ATG16L1 expression in Huh7 cells.

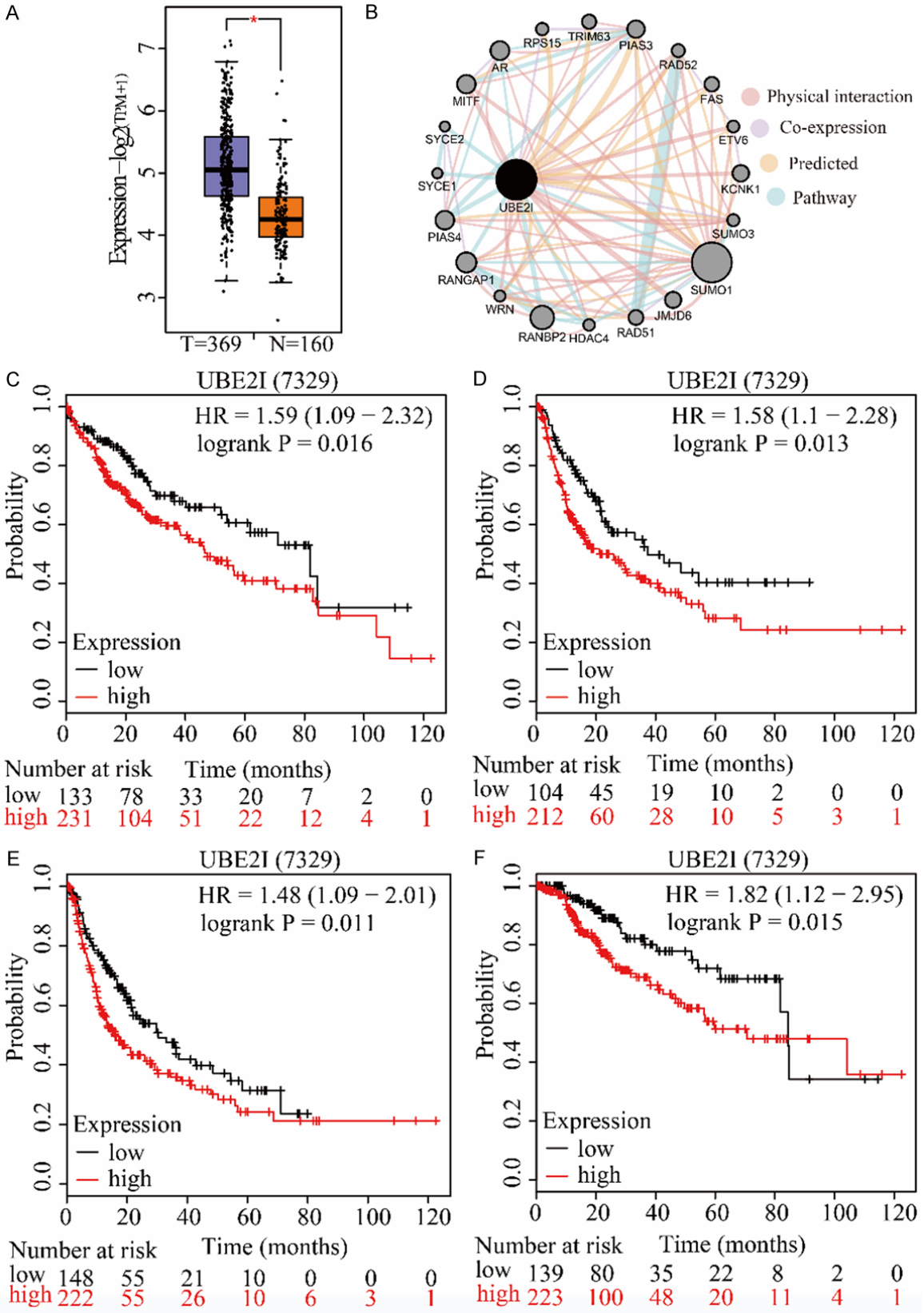

Figure 2. Clinical analysis and interaction network of UBE2I in HCC. A: Differential expression of UBE2I in HCC. B: Gene-gene interaction network of UBE2I and expression-related genes. C-F: Survival analysis of *UBE2I* expression affecting OS (low = 133, high = 231), RFS (low = 104, high = 212), PFS (low = 148, high = 222) and DSS (low = 139, high = 223) in HCC.

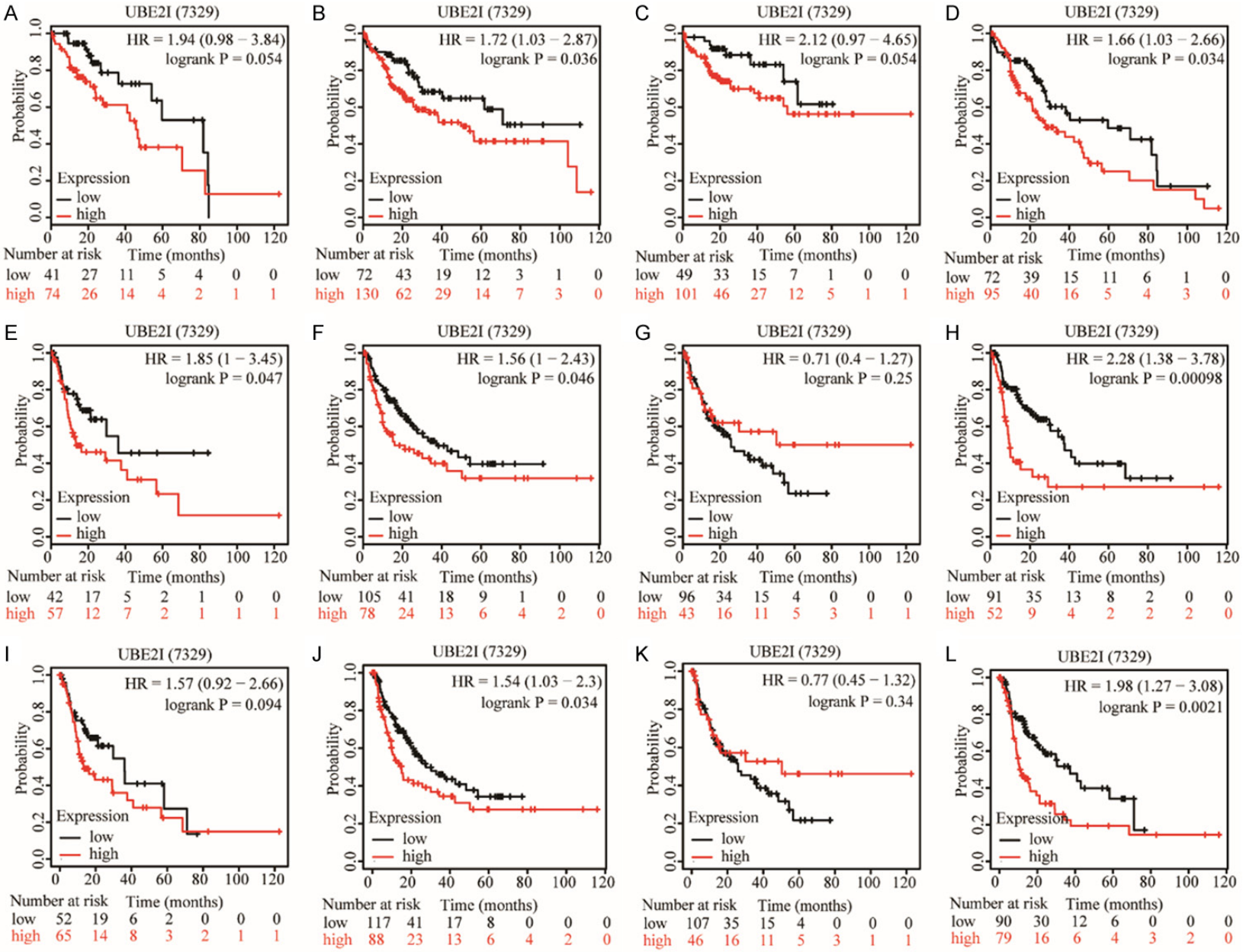
A
UBE2I (7329)
HR = 1.94 (0.98 − 3.84)
logrank P = 0.054
Probability
Expression
low
high
Number at risk
Time (months)
low 41 27 11 5 4 0 0
high 74 26 14 4 2 1 1
B
UBE2I (7329)
HR = 1.72 (1.03 − 2.87)
logrank P = 0.036
Number at risk
low 72 43 19 12 3 1 0
high 130 62 29 14 7 3 0
C
UBE2I (7329)
HR = 2.12 (0.97 − 4.65)
logrank P = 0.054
Number at risk
low 49 33 15 7 1 0 0
high 101 46 27 12 5 1 1
D
UBE2I (7329)
HR = 1.66 (1.03 − 2.66)
logrank P = 0.034
Number at risk
low 72 39 15 11 6 1 0
high 95 40 16 5 4 3 0
E
UBE2I (7329)
HR = 1.85 (1 − 3.45)
logrank P = 0.047
Number at risk
low 42 17 5 2 1 0 0
high 57 12 7 2 1 1 1
F
UBE2I (7329)
HR = 1.56 (1 − 2.43)
logrank P = 0.046
Number at risk
low 105 41 18 9 1 0 0
high 78 24 13 6 4 2 0
G
UBE2I (7329)
HR = 0.71 (0.4 − 1.27)
logrank P = 0.25
Number at risk
low 96 34 15 4 0 0 0
high 43 16 11 5 3 1 1
H
UBE2I (7329)
HR = 2.28 (1.38 − 3.78)
logrank P = 0.00098
Number at risk
low 91 35 13 8 2 0 0
high 52 9 4 2 2 2 0
I
UBE2I (7329)
HR = 1.57 (0.92 − 2.66)
logrank P = 0.094
Number at risk
low 52 19 6 2 0 0 0
high 65 14 8 3 2 1 1
J
UBE2I (7329)
HR = 1.54 (1.03 − 2.3)
logrank P = 0.034
Number at risk
low 117 41 17 8 0 0 0
high 88 23 13 6 4 2 0
K
UBE2I (7329)
HR = 0.77 (0.45 − 1.32)
logrank P = 0.34
Number at risk
low 107 35 15 4 0 0 0
high 46 16 11 5 3 1 1
L
UBE2I (7329)
HR = 1.98 (1.27 − 3.08)
logrank P = 0.0021
Number at risk
low 90 30 12 6 0 0 0
high 79 16 6 4 3 2 0

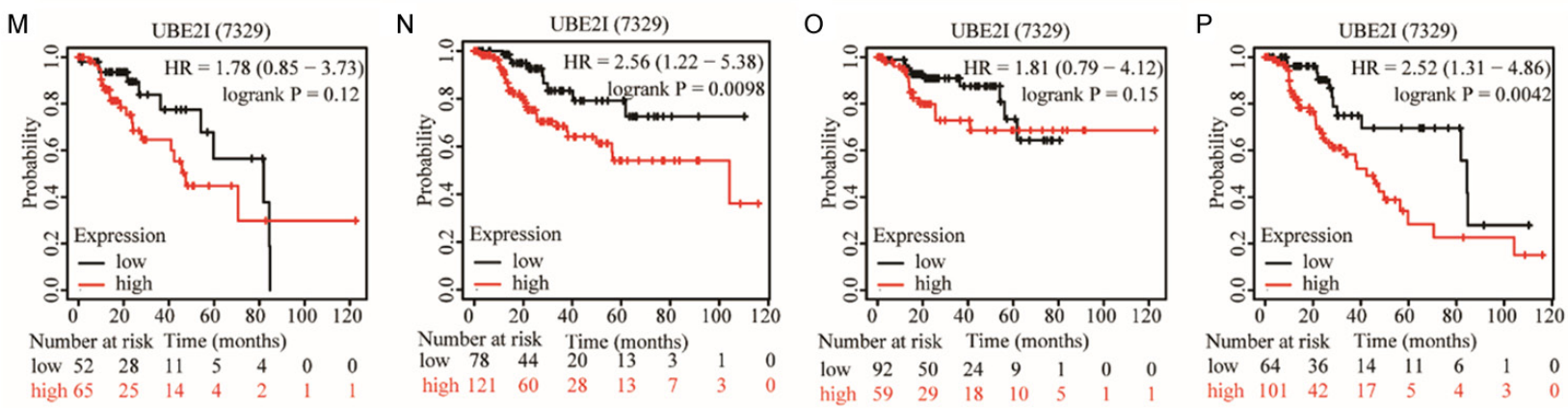

Figure 3. Stratification analysis of UBE2I by alcohol ingestion and hepatitis status in HCC. A, E, I, M: Stratification analysis of UBE2I in a drinking population for OS (low = 41, high = 74), RFS (low = 42, high = 57), PFS (low = 52, high = 65) and DSS (low = 52, high = 65). B, F, J, N: Stratification analysis of UBE2I in a non-drinking population for OS (low = 72, high = 130), RFS (low = 105, high = 78), PFS (low = 117, high = 88) and DSS (low = 78, high = 121). C, G, K, O: Stratification analysis of UBE2I in a hepatitis patient population for OS (low = 49, high = 101), RFS (low = 96, high = 43), PFS (low = 107, high = 46) and DSS (low = 92, high = 59). D, H, L, P: Stratification analysis of UBE2I in a hepatitis-free population for OS (low = 72, high = 95), RFS (low = 91, high = 52), PFS (low = 90, high = 79) and DSS (low = 94, high = 101).

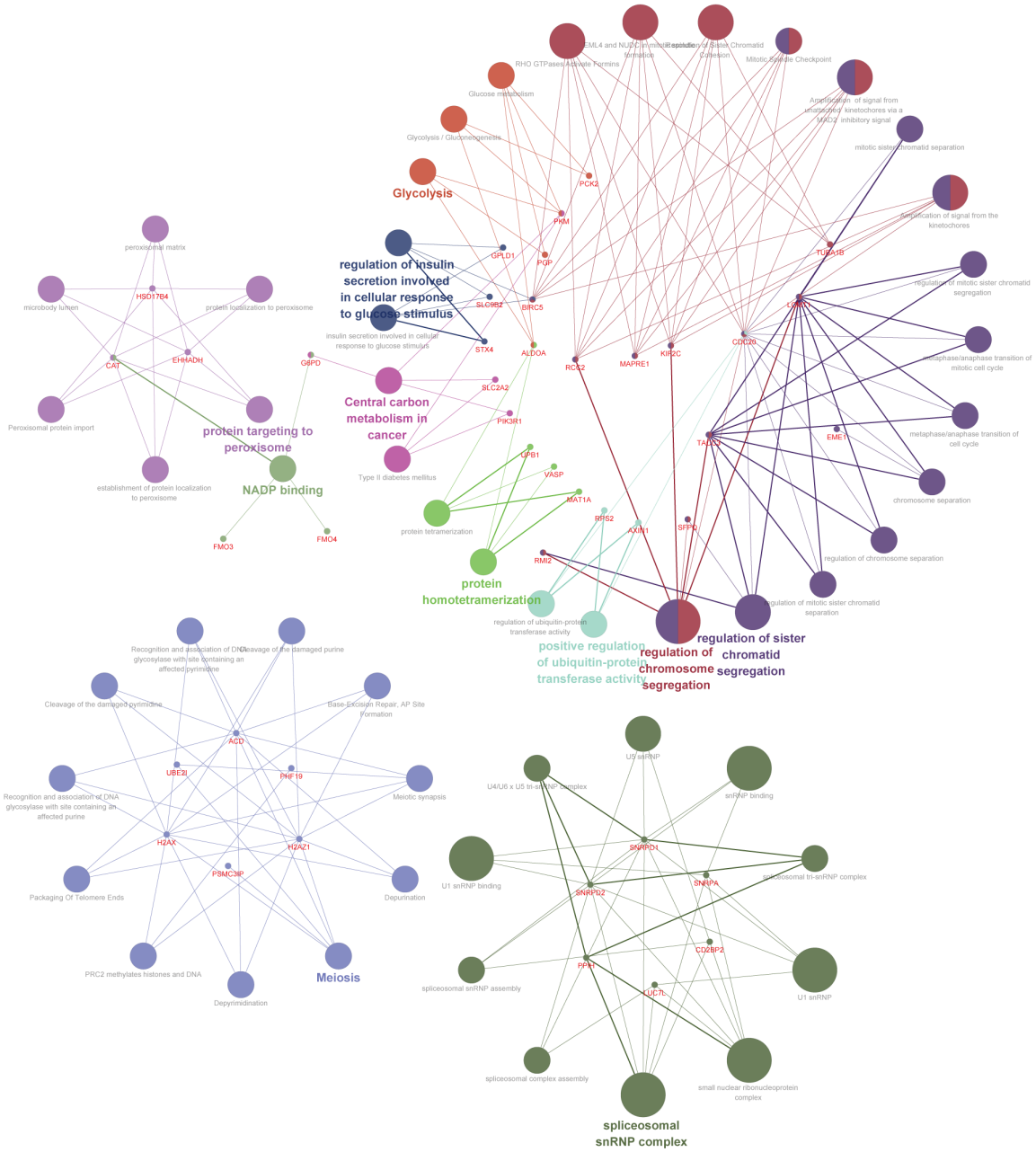

Figure 4. Interaction network of candidate molecular mechanisms involving UBE2I and co-expression-related genes.

Molecular mechanisms underlying UBE2I involvement in HCC by RNA-sequencing

We further examined molecular mechanisms underlying UBE2I involvement in HCC by the RNA-sequencing method. A total of 166 DEGs, including 74 upregulated and 92 downregulated genes, were identified in HCCM cells. Meanwhile, 1883 DEGs, including 845 upregulated and 1038 downregulated genes, were identified in Huh7 cells (**Figure 9A**, **9B**). A total of 27 DEGs intersected in the above two cell lines (**Figure 9C**). Details of DEGs in HCCM and Huh7 cells and intersecting DEGs are shown in Tables S2, S3, S4. Additionally, enrichment of GO terms and KEGG pathways showed the involvement of serine-type endopeptidase inhibitor activity, peptidase regulator activity, organic anion transmembrane transporter activity, extracellular matrix binding, laminin binding, wound healing, high-density lipoprotein particle, regulation of hemostasis, complement and coagulation cascades, among others (**Figure 9D-G**).

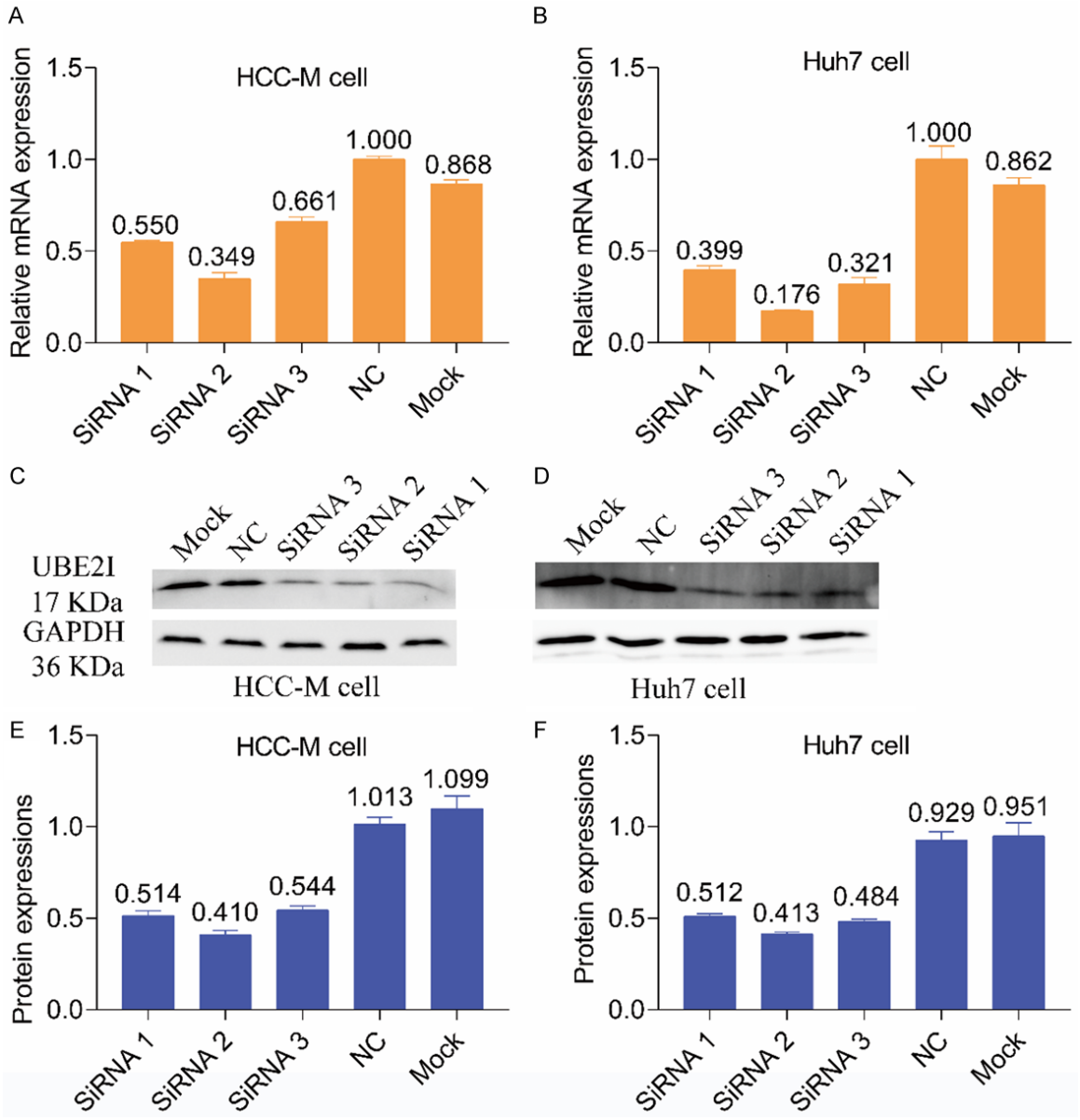

Figure 5. Results of real-time PCR and WB after silencing UBE2I. A, B: Results of real-time PCR after silencing UBE2I in HCCM and Huh7 cells. C, D: Results of WB after silencing UBE2I in HCCM and Huh7 cells. E, F: Histogram showing results of WB after silencing UBE2I in HCCM and Huh7 cells.

We then analyzed enrichment of reactome pathways, DO and DisGeNET. In the reactome pathway, we saw enrichment of perioximal protein import, plasma lipoprotein assembly, remodeling, formation of fibrin clot (clotting cascade), platelet degranulation, metabolism of vitamins and cofactors (**Figure 10A**, **10B**). In DO, there was enrichment of liver disease, hepatitis, fatty liver disease, bile duct disease, biliary duct disease, obesity, lipid storage disease, type 2 mellitus diabetes and pancreas disease (**Figure 10C**, **10D**). In DisGeNET, enrichment was seen for hepatocarcinogenesis, tumor angiogenesis, inflammation, steatohepatitis, fatty liver, non-alcoholic fatty liver disease, hepatoblastoma and liver fibrosis (**Figure 10E**, **10F**).

Discussion

SUMO is a highly conserved protein family that is involved in protein modification after translation [28]. Although similar to ubiquitination in several aspects such as structure, conjugation process and attachment to targets, SUMOylation is different from ubiquitination in its biological consequences [28]. SUMOylation

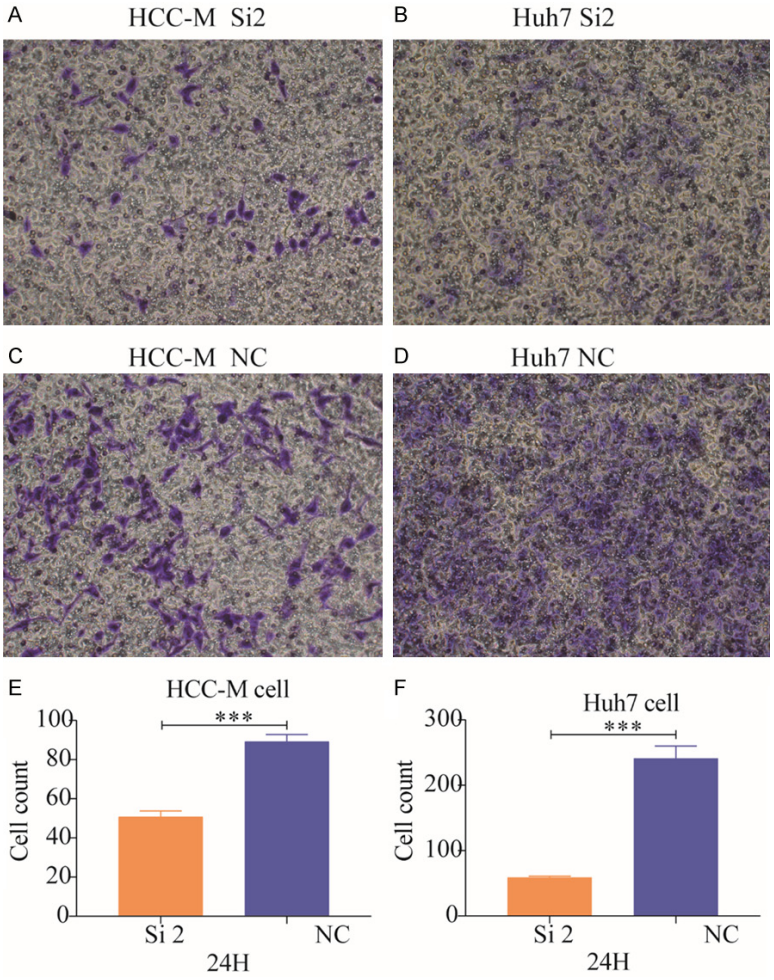

Figure 6. Results of cell invasion assays. A, B: Results of cell invasion assays in the siRNA-2 groups of HCCM and Huh7 cells. C, D: Results of cell invasion assays in the negative control groups for HCCM and Huh7 cells. E, F: Histograms comparing the two groups of HCCM and Huh7 cells.

has been implicated in the modulation of transcriptional activity, protein activity, subcellular localization and protein-protein interactions [29, 30]. The ubiquitination pathway employs many kinds of E2-conjugating enzymes for its metabolism [9]. In contrast, UBE2I is the only known E2-conjugating enzyme in the SUMO pathway and has been documented in yeast, invertebrates and vertebrates [31-33]. SUMOylation modulates a great number of cellular processes such as DNA replication and repair, chromosome integrity and segregation, signal transduction, cell cycle progression and nuclear transport, among others [34-37]. In agreement with previous reports, our study showed that UBE2I and its co-expression-related genes participated in protein targeting to peroxisome, NADP binding, central carbon metabolism in cancer, meiosis, protein homotetramerization, positive regulation of ubiquitin-protein transferase activity, regulation of chromosome segregation, regulation of sister chromatid segregation, glycolysis and regulation of insulin secretion involved in cellular response to glucose stimulus.

More recently, research has demonstrated that UBE2I can play an important role without relying on SUMOylation to regulate cell growth [38, 39]. These studies suggested that changing UBE2I expression could influence cell growth and functions. For instance, Beck et al. suggested that overexpression of a UBE2I dominant-negative mutant was linked to increased drug sensitivity in breast cancer [40]. In yeast, defects in UBE2I expression induce increased sensitivity to genotoxic drugs [41]. In breast cancer, Mo et al. showed evidence that *UBE2I* promoted metastasis and invasion in a SUMOylation-independent manner via downregulation of a putative tumor suppressor microRNA-224 [42]. Su et al. suggested that high expression of UBE2I was correlated with poor response to chemotherapy and poor prognosis [43]. These research studies consistently indicate an oncogenic role for UBE2I expression in breast cancer.

In lung cancer research, He et al. demonstrated that high expression of UBE2I led to increased cell migration and invasion and suggested that it plays a pivotal role in lung cancer by promoting cell migration and invasion [43]. In osteosarcoma, Wu et al. revealed that downregulation of UBE2I suppressed tumorigenesis and enhanced chemosensitivity to HSV-TK/GCV by modulating connexin-43 SUMOylation [44]. Ran et al. found that UBE2I expression played a pivotal role in tumorigene-

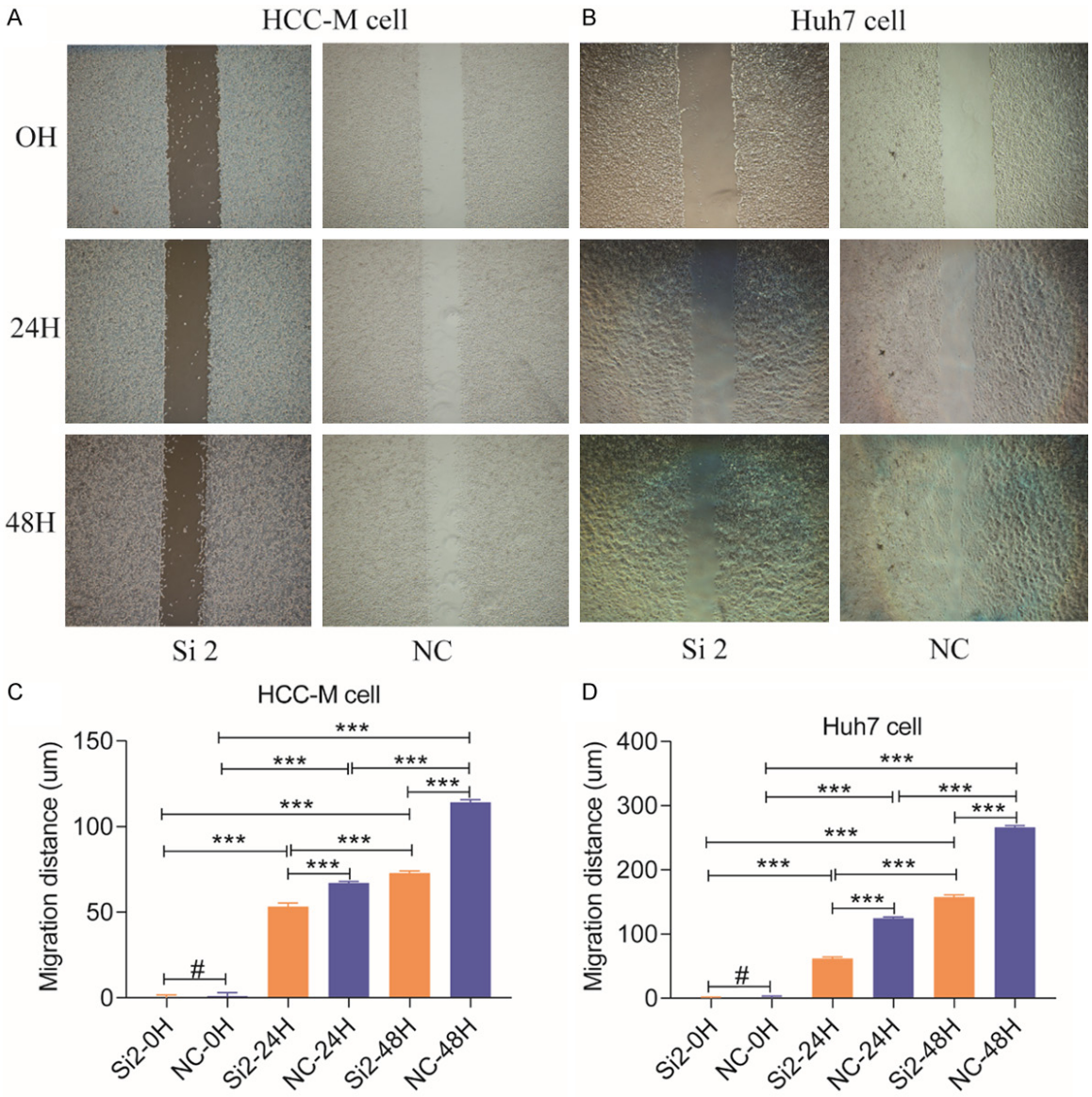

Figure 7. Results of cell migration assays. A, B: Results of cell invasion assays of HCCM and Huh7 cells. C, D: Histograms comparing the two groups of HCCM and Huh7 cells at 0, 24 and 48 h.

sis and tumor progression of squamous cell carcinoma of the head and neck [45]. Shengkui et al. examined aberrant expression of microRNA-214 and UBE2I and found that high expression of UBE2I and low expression of microRNA-214 was associated with the poorest OS and was an independent prognostic predictor of glioma [15]. Their further stratification analysis demonstrated that high expression of UBE2I and low expression of microRNA-214 were obviously correlated with poor OS of glioma patients with high pathological grades [15]. The above studies thus suggested an oncogenic role for UBE2I expression in these malignancies. Parallel with them, we revealed an oncogenic role of UBE2I affecting HCC prognosis as assessed by OS, RFS, PFS and DSS. In addition, stratification analysis according to alcohol ingestion and hepatitis status suggested that high expression of UBE2I was an indicator of poor prognosis in HCC as well.

Autophagy is a catabolic mechanism and influences the growth of tumor cells. Autophagy maintains body development, aging and degeneration like a two-edged sword according to its changing activity [46]. Autophagy has been implicated as a disease-associated fac-

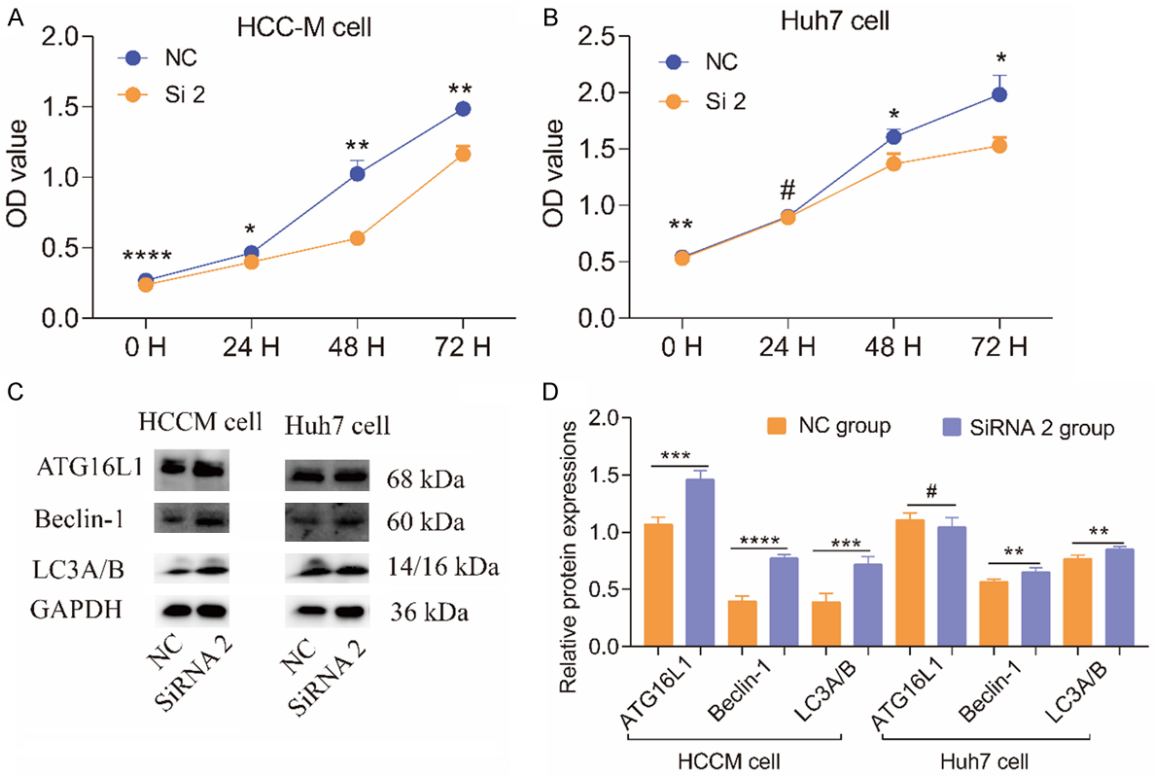

Figure 8. Results of cell proliferation assays and WB results of autophagy pathway-related proteins. A, B: Results of cell proliferation assays of HCCM and Huh7 cells at 0, 24, 48 and 72 h. C: WB results of autophagy pathway-related proteins. D: Histogram comparing autophagy pathway-related proteins in HCCM and Huh7 cells.

tor that is regulated in the liver cells of humans with liver diseases and accounts for the development and progression of various liver diseases such as hepatitis, steatosis, fibrosis, cirrhosis and HCC [47-50]. Autophagy protects liver cells from injury and cell death by eliminating injured organelles and proteins associated with liver diseases [51]. Beclin-1 is a key protein in the formation of autophagosomes [52]. LC3-I is transformed to LC3-II during autophagy and an increase in the LC3-II/LC3-I ratio indicates an enhancement of autophagy levels [53].

Jiang's study focused on the role of matrine in HCC and showed that matrine could inhibit cell proliferation, migration and invasion and promote autophagy in HCC by regulating the circ_0027345/miR-345-5P/HOXD3 axis [54]. In agreement with this study, our research showed that silencing UBE2I expression led to decreased cell migration, invasion and proliferation and promoted protein expression of LC3A/B, Beclin-1 and ATG16L1 in the autophagy pathway in HCC cells. By inhibiting UBE2I expression to decrease the IC50 value of doxorubicin in HCC cells, Guo et al. showed that downregulating UBE2I could increase the sensitivity of HCC to doxorubicin [28]. They further demonstrated that downregulation of UBE2I has an apparent effect on the mitogen-activated protein kinase signaling pathway [28]. Recently, Lou et al. found that UBE2I promotes metastasis and was correlated with poor prognosis in HCC [55]. They suggested that downregulating UBE2I expression significantly inhibited the migration and invasion of HCC cells. Consistent with their results, our study found that knockdown of UBE2I decreased cell migration, invasion and proliferation. In addition, Lu et al. showed that loss of inhibition by has-miR-195-3P and dysregulation of UBE2I promoter methylation were associated with the overexpression of UBE2I in HCC. In contrast, we explored whether changing UBE2I expression influenced expression of autophagy pathway-related proteins and found that UBE2I knockdown was associated with high expression of autophagy pathway-related proteins, including LC3A/B, Beclin-1 and ATG16L1 in HCC cells.

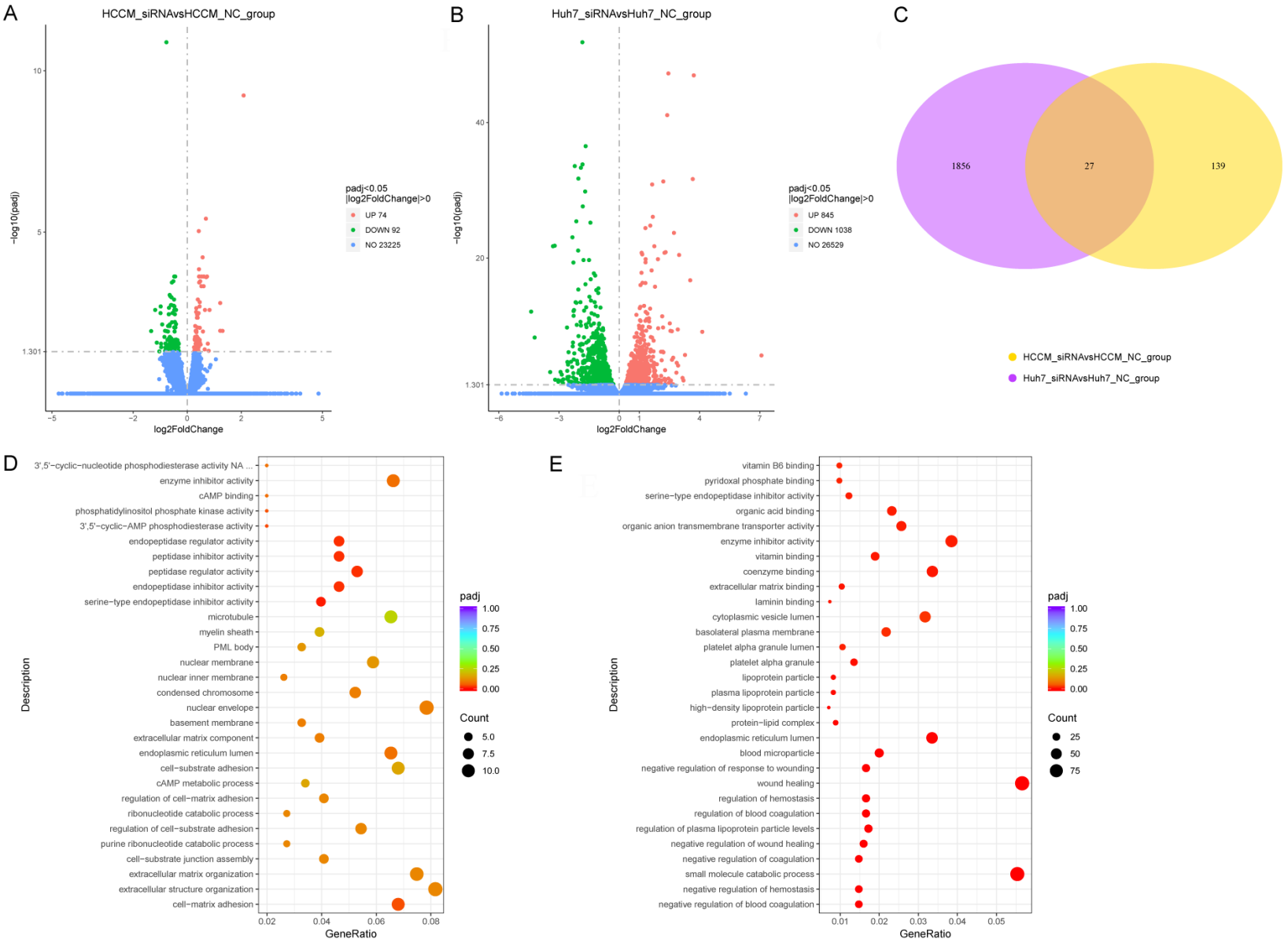
A
HCCM_siRNAvsHCCM_NC_group
−log10(padj)
log2FoldChange
padj<0.05
|log2FoldChange|>0
UP 74
DOWN 92
NO 23225
B
Huh7_siRNAvsHuh7_NC_group
−log10(padj)
log2FoldChange
padj<0.05
|log2FoldChange|>0
UP 845
DOWN 1038
NO 26529
C
1856
27
139
HCCM_siRNAvsHCCM_NC_group
Huh7_siRNAvsHuh7_NC_group
D
3',5'−cyclic−nucleotide phosphodiesterase activity NA ...
enzyme inhibitor activity
cAMP binding
phosphatidylinositol phosphate kinase activity
3',5'−cyclic−AMP phosphodiesterase activity
endopeptidase regulator activity
peptidase inhibitor activity
peptidase regulator activity
endopeptidase inhibitor activity
serine−type endopeptidase inhibitor activity
microtubule
myelin sheath
PML body
nuclear membrane
nuclear inner membrane
condensed chromosome
nuclear envelope
basement membrane
extracellular matrix component
endoplasmic reticulum lumen
cell−substrate adhesion
cAMP metabolic process
regulation of cell−matrix adhesion
ribonucleotide catabolic process
regulation of cell−substrate adhesion
purine ribonucleotide catabolic process
cell−substrate junction assembly
extracellular matrix organization
extracellular structure organization
cell−matrix adhesion
Description
GeneRatio
padj
Count
E
vitamin B6 binding
pyridoxal phosphate binding
serine−type endopeptidase inhibitor activity
organic acid binding
organic anion transmembrane transporter activity
enzyme inhibitor activity
vitamin binding
coenzyme binding
extracellular matrix binding
laminin binding
cytoplasmic vesicle lumen
basolateral plasma membrane
platelet alpha granule lumen
platelet alpha granule
lipoprotein particle
plasma lipoprotein particle
high−density lipoprotein particle
protein−lipid complex
endoplasmic reticulum lumen
blood microparticle
negative regulation of response to wounding
wound healing
regulation of hemostasis
regulation of blood coagulation
regulation of plasma lipoprotein particle levels
negative regulation of wound healing
negative regulation of coagulation
small molecule catabolic process
negative regulation of hemostasis
negative regulation of blood coagulation
Description
GeneRatio
padj
Count

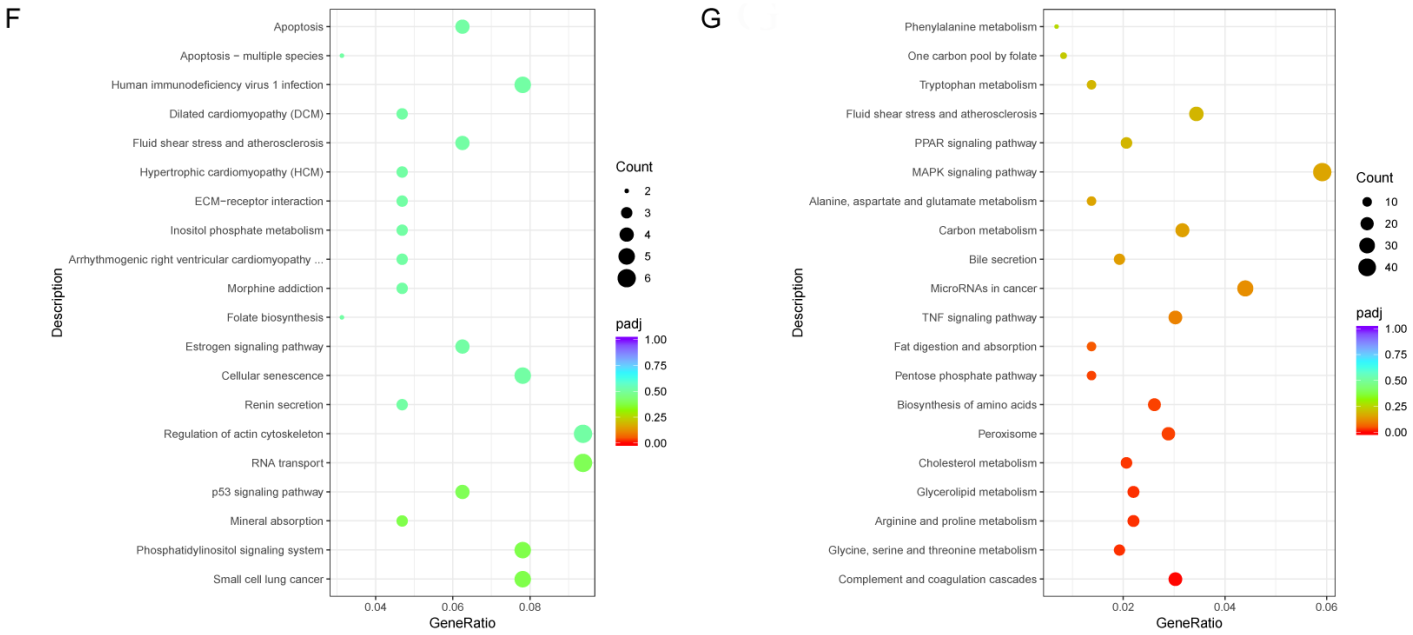

Figure 9. Volcano plots, Venn diagram and dot plots based on DEGs in HCCM and Huh7 cells. A, B: Volcano plots in HCCM and Huh7 cells. C: Venn diagram of DEGs in HCCM and Huh7 cells. D, E: Dot plots showing enrichment of GO terms in HCCM and Huh7 cells. F, G: Dot plots showing enriched KEGG pathways in HCCM and Huh7 cells.

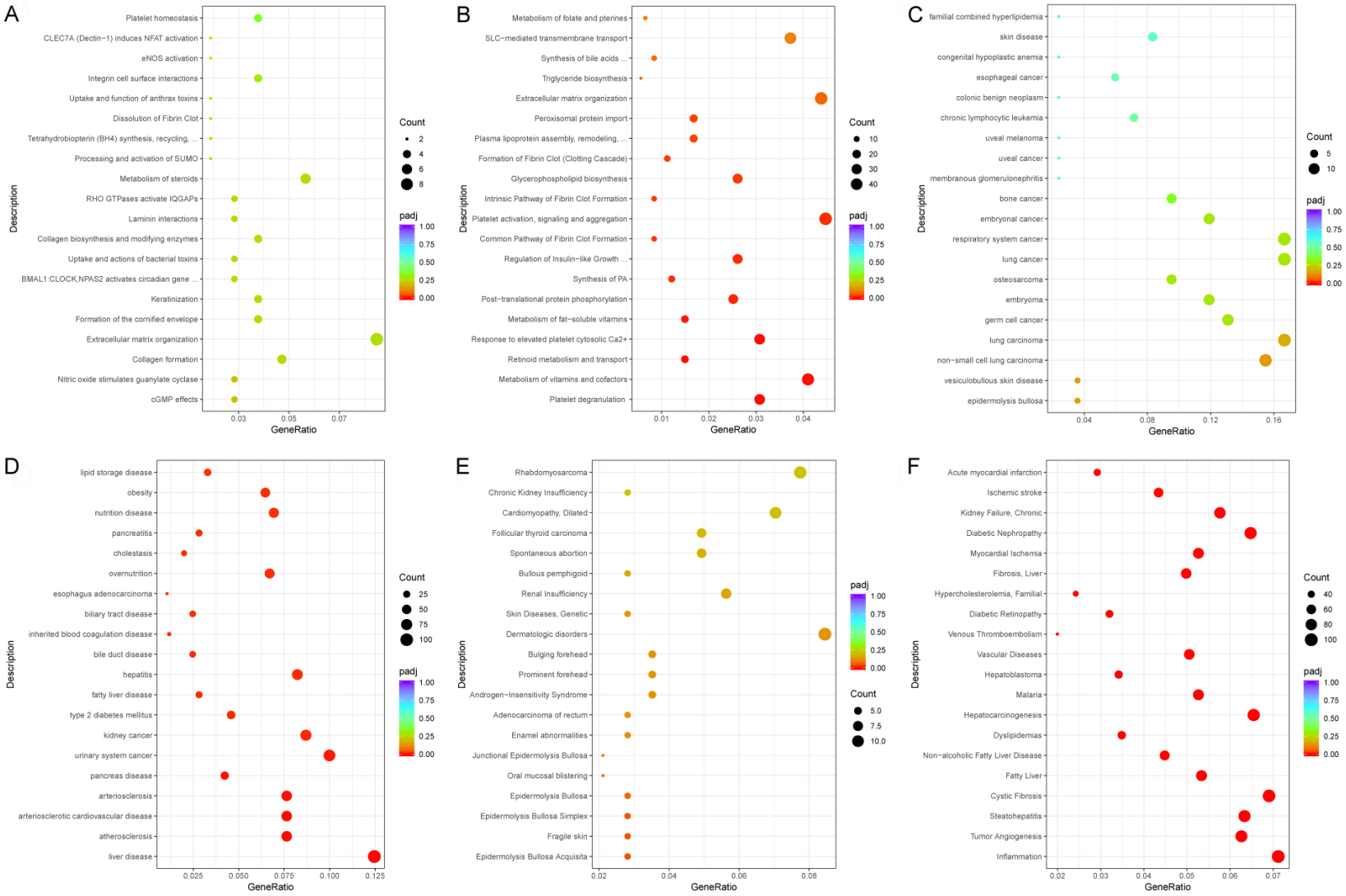

Figure 10. Dot plots of enrichment analysis results for the reactome pathway, disease ontology and DisGeNET. A, B: Dot plots of enrichment analysis results for reactome pathways in HCCM and Huh7 cells. C, D: Dot plots of enrichment analysis results for disease ontology in HCCM and Huh7 cells. E, F: Dot plots of enrichment analysis results for DisGeNET in HCCM and Huh7 cells.

Furthermore, we explored possible molecular mechanisms of UBE2I using the RNA-sequencing method. RNA-sequencing results indicated enrichment in GO terms and KEGG pathways involving serine-type endopeptidase inhibitor activity, peptidase regulator activity, organic anion transmembrane transporter activity, extracellular matrix binding, laminin binding, wound healing, high-density lipoprotein particle, regulation of hemostasis, complement and coagulation cascades. Enrichment analysis including the reactome pathway, DO, and DisGeNET was then performed. Results suggested involvement in hepatocarcinogenesis, tumor angiogenesis, inflammation, steatohepatitis, fatty liver, non-alcoholic fatty liver disease, hepatoblastoma, liver fibrosis, hepatitis, biliary duct disease, obesity, lipid storage disease, type 2 mellitus diabetes, pancreas disease, perioximal protein import, plasma lipoprotein assembly and remodeling. To date, a great deal of research has focused on non-alcohol fatty liver disease [56], liver fibrosis [57, 58], hepatitis [59], steotohepatitis [60, 61], obesity [62] and type 2 diabetes mellitus [63] and has implicated them in the occurrence and progression of HCC. Therefore, we have good reasons to believe that UBE2I may be involved in HCC through its relationship with the above diseases. However, this hypothesis needs further validation.

There were some limitations in the study that should be recognized. First, in vivo experiments need to be performed to explore the molecular mechanisms. Second, RNA-sequencing results need to be further validated in future studies. Third, associations between UBE2I expression and clinical pathological factors should be investigated. Then, relationship between overexpression of UBE2I and cell lines should further be attempted to validate. Moreover, RNA-sequencing results should be verified in the near future work.

Conclusion

We found that UBE2I was not only differentially expressed in HCC but also showed prognostic significance and association with immune infiltrates in HCC. In vitro experiments demonstrated that high expression of UBE2I was associated with increased cell migration, invasion and proliferation of HCC cells. WB indicated that downregulated expression of UBE2I was negatively correlated with higher expression of autophagy pathway proteins. Furthermore, we conducted RNA-sequencing after silencing UBE2I and found that it participated in the process of hepatocarcinogenesis, tumor angiogenesis, inflammation, steatohepatitis, non-alcoholic fatty liver disease, liver fibrosis, hepatitis, obesity, lipid storage disease, type 2 mellitus diabetes and others. Further validation of these results is warranted in future studies.

Acknowledgements

This work was supported in part by the National Natural Science Foundation of China (No.: 81560535, 81802874), Natural Science Foundation of Guangxi Province of China (Grant No. 2018GXNSFBA138013, 2018GXNSFAA050119, 2020GXNSFAA159127), Key laboratory of High-Incidence-Tumor Prevention & Treatment (Guangxi Medical University), Ministry of Education (GKE2018-01, GKE2019-11, GKEZZ202009), The Basic Ability Improvement Project for Middle-aged and Young Teachers in Colleges and Universities in Guangxi (2018KY0110), Guangxi Key Laboratory for the Prevention and Control of Viral Hepatitis (No. GXCDCKL201902), and 2018 Innovation Project of Guangxi Graduate Education (JGY2018037). As well as, the present study is also partly supported by Research Institute of Innovative Think-tank in Guangxi Medical University (The gene-environment interaction in hepatocarcinogenesis in Guangxi HCCs and its translational applications in the HCC prevention) and The central government in 2019 subsidized Guangxi's major and difficult disease clinical collaboration construction project of Chinese and Western medicine. We would also acknowledge the supported by the Key laboratory of High-Incidence-Tumor Prevention & Treatment (Guangxi Medical University), Ministry of Education. This article does not contain any studies with human participants or animals performed by any of the authors.

Disclosure of conflict of interest

None.

Address correspondence to: Drs. Tao Peng and Guang-Zhi Zhu, Department of Hepatobiliary Surgery, The First Affiliated Hospital of Guangxi Medical University, Nanning 530021, Guangxi Province, China. Tel: +86-771-5356528; Fax: +86-771-5350031; E-mail: pengtaogmu@163.com (TP); zhuguangzhi0792@hotmail.com (GZZ)

References

[1] Chen J, Zhang ZQ, Song J, Liu QM, Wang C, Huang Z, Chu L, Liang HF, Zhang BX and Chen XP. 18beta-glycyrrhetinic-acid-mediated unfolded protein response induces autophagy and apoptosis in hepatocellular carcinoma. Sci Rep 2018; 8: 9365.

[2] Forner A, Llovet JM and Bruix J. Hepatocellular carcinoma. Lancet 2012; 379: 1245-1255.

[3] El-Serag HB. Epidemiology of viral hepatitis and hepatocellular carcinoma. Gastroenterology 2012; 142: 1264-1273, e1261.

[4] Chen C and Wang G. Mechanisms of hepatocellular carcinoma and challenges and opportunities for molecular targeted therapy. World J Hepatol 2015; 7: 1964-1970.

[5] Villanueva A and Llovet JM. Liver cancer in 2013: mutational landscape of HCC–the end of the beginning. Nat Rev Clin Oncol 2014; 11: 73-74.

[6] Levi Sandri GB, de Werra E, Mascianà G, Colasanti M, Santoro R, D'Andrea V and Ettorre GM. Laparoscopic and robotic approach for hepatocellular carcinoma-state of the art. Hepatobiliary Surg Nutr 2016; 5: 478-484.

[7] Toyoda H, Kumada T, Tada T, Ito T, Maeda A, Kaneoka Y, Kagebayashi C and Satomura S. Changes in highly sensitive alpha-fetoprotein for the prediction of the outcome in patients with hepatocellular carcinoma after hepatectomy. Cancer Med 2014; 3: 643-651.

[8] Gill G. SUMO and ubiquitin in the nucleus: different functions, similar mechanisms? Genes Dev 2004; 18: 2046-2059.

[9] Hochstrasser M. Origin and function of ubiquitin-like proteins. Nature 2009; 458: 422-429.

[10] Geiss-Friedlander R and Melchior F. Concepts in sumoylation: a decade on. Nat Rev Mol Cell Biol 2007; 8: 947-956.

[11] Tahmasebi S, Ghorbani M, Savage P, Gocevski G and Yang XJ. The SUMO conjugating enzyme Ubc9 is required for inducing and maintaining stem cell pluripotency. Stem Cells 2014; 32: 1012-1020.

[12] Koh EH, Chen Y, Bader DA, Hamilton MP, He B, York B, Kajimura S, McGuire SE and Hartig SM. Mitochondrial activity in human white adipocytes is regulated by the ubiquitin carrier protein 9/microRNA-30a axis. J Biol Chem 2016; 291: 24747-24755.

[13] Li H, Niu H, Peng Y, Wang J and He P. Ubc9 promotes invasion and metastasis of lung cancer cells. Oncol Rep 2013; 29: 1588-1594.

[14] Dong M, Pang X, Xu Y, Wen F and Zhang Y. Ubiquitin-conjugating enzyme 9 promotes epithelial ovarian cancer cell proliferation in vitro. Int J Mol Sci 2013; 14: 11061-11071.

[15] Wang S, Jiao B, Geng S, Ma S, Liang Z and Lu S. Combined aberrant expression of microRNA-214 and UBC9 is an independent unfavorable prognostic factor for patients with gliomas. Med Oncol 2014; 31: 767.

[16] Li T, Fan J, Wang B, Traugh N, Chen Q, Liu JS, Li B and Liu XS. TIMER: a web server for comprehensive analysis of tumor-infiltrating immune cells. Cancer Res 2017; 77: e108-e110.

[17] Li B, Severson E, Pignon JC, Zhao H, Li T, Novak J, Jiang P, Shen H, Aster JC, Rodig S, Signoretti S, Liu JS and Liu XS. Comprehensive analyses of tumor immunity: implications for cancer immunotherapy. Genome Biol 2016; 17: 174.

[18] Lian Q, Wang S, Zhang G, Wang D, Luo G, Tang J, Chen L and Gu J. HCCDB: a database of hepatocellular carcinoma expression atlas. Genomics Proteomics Bioinformatics 2018; 16: 269-275.

[19] Tang Z, Li C, Kang B, Gao G, Li C and Zhang Z. GEPIA: a web server for cancer and normal gene expression profiling and interactive analyses. Nucleic Acids Res 2017; 45: W98-w102.

[20] Menyhárt O, Nagy Á and Győrffy B. Determining consistent prognostic biomarkers of overall survival and vascular invasion in hepatocellular carcinoma. R Soc Open Sci 2018; 5: 181006.

[21] Montojo J, Zuberi K, Rodriguez H, Kazi F, Wright G, Donaldson SL, Morris Q and Bader GD. GeneMANIA Cytoscape plugin: fast gene function predictions on the desktop. Bioinformatics 2010; 26: 2927.

[22] Shannon P, Markiel A, Ozier O, Baliga NS, Wang JT, Ramage D, Amin N, Schwikowski B and Ideker T. Cytoscape: a software environment for integrated models of biomolecular interaction networks. Genome Res 2003; 13: 2498.

[23] Bindea G, Mlecnik B, Hackl H, Charoentong P, Tosolini M, Kirilovsky A, Fridman WH, Pagès F, Trajanoski Z and Galon J. ClueGO: a cytoscape plug-in to decipher functionally grouped gene ontology and pathway annotation networks. Bioinformatics (Oxford, England) 2009; 25: 1091-1093.

[24] Cerami E, Gao J, Dogrusoz U, Gross BE, Sumer SO, Aksoy BA, Jacobsen A, Byrne CJ, Heuer ML, Larsson E, Antipin Y, Reva B, Goldberg AP, Sander C and Schultz N. The cBio cancer genomics portal: an open platform for exploring multidimensional cancer genomics data. Cancer Discov 2012; 2: 401-404.

[25] Gao J, Aksoy BA, Dogrusoz U, Dresdner G, Gross B, Sumer SO, Sun Y, Jacobsen A, Sinha R, Larsson E, Cerami E, Sander C and Schultz N. Integrative analysis of complex cancer genomics and clinical profiles using the cBioPortal. Sci Signal 2013; 6: pl1.

[26] Lu GD, Leung CH, Yan B, Tan CM, Low SY, Aung MO, Salto-Tellez M, Lim SG and Hooi SC. C/EB-Palpha is up-regulated in a subset of hepatocellular carcinomas and plays a role in cell growth and proliferation. Gastroenterology 2010; 139: 632-43, 643.e1-4.
[27] Love MI, Huber W and Anders S. Moderated estimation of fold change and dispersion for RNA-seq data with DESeq2. Genome Biol 2014; 15: 550.
[28] Fang S, Qiu J, Wu Z, Bai T and Guo W. Down-regulation of UBC9 increases the sensitivity of hepatocellular carcinoma to doxorubicin. Oncotarget 2017; 8: 49783-49795.
[29] Müller S, Hoege C, Pyrowolakis G and Jentsch S. SUMO, ubiquitin's mysterious cousin. Nat Rev Mol Cell Biol 2001; 2: 202-210.
[30] Zhou F, Xue Y, Lu H, Chen G and Yao X. A genome-wide analysis of sumoylation-related biological processes and functions in human nucleus. FEBS Lett 2005; 579: 3369-3375.
[31] Desterro JM, Thomson J and Hay RT. Ubch9 conjugates SUMO but not ubiquitin. FEBS Lett 1997; 417: 297-300.
[32] Hayashi T, Seki M, Maeda D, Wang W, Kawabe Y, Seki T, Saitoh H, Fukagawa T, Yagi H and Enomoto T. Ubc9 is essential for viability of higher eukaryotic cells. Exp Cell Res 2002; 280: 212-221.
[33] Johnson ES and Blobel G. Ubc9p is the conjugating enzyme for the ubiquitin-like protein Smt3p. J Biol Chem 1997; 272: 26799-26802.
[34] Seeler JS and Dejean A. Nuclear and unclear functions of SUMO. Nat Rev Mol Cell Biol 2003; 4: 690-699.
[35] Johnson ES. Protein modification by SUMO. Annu Rev Biochem 2004; 73: 355-382.
[36] Zhao J. Sumoylation regulates diverse biological processes. Cell Mol Life Sci 2007; 64: 3017-3033.
[37] Li YJ, Stark JM, Chen DJ, Ann DK and Chen Y. Role of SUMO: SIM-mediated protein-protein interaction in non-homologous end joining. Oncogene 2010; 29: 3509-3518.
[38] Guo Y, Yang MC, Weissler JC and Yang YS. Modulation of PLAGL2 transactivation activity by Ubc9 co-activation not SUMOylation. Biochem Biophys Res Commun 2008; 374: 570-575.
[39] Kaul S, Blackford JA Jr, Cho S and Simons SS Jr. Ubc9 is a novel modulator of the induction properties of glucocorticoid receptors. J Biol Chem 2002; 277: 12541-12549.
[40] Mo YY, Yu Y, Ee PL and Beck WT. Overexpression of a dominant-negative mutant Ubc9 is associated with increased sensitivity to anticancer drugs. Cancer Res 2004; 64: 2793-2798.
[41] Jacquiau HR, van Waardenburg RC, Reid RJ, Woo MH, Guo H, Johnson ES and Bjornsti MA. Defects in SUMO (small ubiquitin-related modifier) conjugation and deconjugation alter cell sensitivity to DNA topoisomerase I-induced DNA damage. J Biol Chem 2005; 280: 23566-23575.
[42] Zhu S, Sachdeva M, Wu F, Lu Z and Mo YY. Ubc9 promotes breast cell invasion and metastasis in a sumoylation-independent manner. Oncogene 2010; 29: 1763-1772.
[43] Chen SF, Gong C, Luo M, Yao HR, Zeng YJ and Su FX. Ubc9 expression predicts chemoresistance in breast cancer. Chin J Cancer 2011; 30: 638-644.
[44] Zhang D, Yu K, Yang Z, Li Y, Ma X, Bian X, Liu F, Li L, Liu X and Wu W. Silencing Ubc9 expression suppresses osteosarcoma tumorigenesis and enhances chemosensitivity to HSV-TK/GCV by regulating connexin 43 SUMOylation. Int J Oncol 2018; 53: 1323-1331.
[45] Ronen O, Malone JP, Kay P, Bivens C, Hall K, Paruchuri LP, Mo YY, Robbins KT and Ran S. Expression of a novel marker, Ubc9, in squamous cell carcinoma of the head and neck. Head Neck 2009; 31: 845-855.
[46] Wang Z and Choi ME. Autophagy in kidney health and disease. Antioxid Redox Signal 2014; 20: 519-537.
[47] Ueno T and Komatsu M. Autophagy in the liver: functions in health and disease. Nat Rev Gastroenterol Hepatol 2017; 14: 170-184.
[48] Wang K. Autophagy and apoptosis in liver injury. Cell Cycle 2015; 14: 1631-1642.
[49] Czaja MJ. Functions of autophagy in hepatic and pancreatic physiology and disease. Gastroenterology 2011; 140: 1895-1908.
[50] Rautou PE, Mansouri A, Lebrec D, Durand F, Valla D and Moreau R. Autophagy in liver diseases. J Hepatol 2010; 53: 1123-1134.
[51] Ke PY. Diverse functions of autophagy in liver physiology and liver diseases. Int J Mol Sci 2019; 20: 300.
[52] Pattingre S, Tassa A, Qu X, Garuti R, Liang XH, Mizushima N, Packer M, Schneider MD and Levine B. Bcl-2 antiapoptotic proteins inhibit Beclin 1-dependent autophagy. Cell 2005; 122: 927-939.
[53] Tanida I, Ueno T and Kominami E. LC3 conjugation system in mammalian autophagy. Int J Biochem Cell Biol 2004; 36: 2503-2518.
[54] Lin S, Zhuang J, Zhu L and Jiang Z. Matrine inhibits cell growth, migration, invasion and promotes autophagy in hepatocellular carcinoma by regulation of circ_0027345/miR-345-5p/HOXD3 axis. Cancer Cell Int 2020; 20: 246.
[55] Yang H, Gao S, Chen J and Lou W. UBE2I promotes metastasis and correlates with poor prognosis in hepatocellular carcinoma. Cancer Cell Int 2020; 20: 234.
[56] Younossi Z, Stepanova M, Ong JP, Jacobson IM, Bugianesi E, Duseja A, Eguchi Y, Wong VW, Ne-

gro F, Yilmaz Y, Romero-Gomez M, George J, Ahmed A, Wong R, Younossi I, Ziayee M and Afendy A. Nonalcoholic steatohepatitis is the fastest growing cause of hepatocellular carcinoma in liver transplant candidates. Clin Gastroenterol Hepatol 2019; 17: 748-755, e743.

[57] Younossi Z and Henry L. Contribution of alcoholic and nonalcoholic fatty liver disease to the burden of liver-related morbidity and mortality. Gastroenterology 2016; 150: 1778-1785.

[58] Kim D, Li AA, Perumpail BJ, Gadiparthi C, Kim W and Cholankeril G. Changing trends in etiology-based and ethnicity-based annual mortality rates of cirrhosis and hepatocellular carcinoma in the United States. Hepatology 2019; 69: 1064-1074.

[59] Marengo A, Rosso C and Bugianesi E. Liver cancer: connections with obesity, fatty liver, and cirrhosis. Annu Rev Med 2016; 67: 103-117.

[60] Younossi ZM, Stepanova M, Rafiq N, Makhlouf H, Younoszai Z, Agrawal R and Goodman Z. Pathologic criteria for nonalcoholic steatohepatitis: interprotocol agreement and ability to predict liver-related mortality. Hepatology 2011; 53: 1874-1882.

[61] Younossi ZM, Stepanova M, Rafiq N, Henry L, Loomba R, Makhlouf H and Goodman Z. Nonalcoholic steatofibrosis independently predicts mortality in nonalcoholic fatty liver disease. Hepatol Commun 2017; 1: 421-428.

[62] Calle EE, Rodriguez C, Walker-Thurmond K and Thun MJ. Overweight, obesity, and mortality from cancer in a prospectively studied cohort of U.S. adults. N Engl J Med 2003; 348: 1625-1638.

[63] Wainwright P, Scorletti E and Byrne C. Type 2 diabetes and hepatocellular carcinoma: risk factors and pathogenesis. Curr Diab Rep 2017; 17: 20.

Table S1. Top 100 genes of UBE2I co-expression related

Correlated Gene	Cytoband	Spearman's Correlation	*p*-Value	q-Value
RNPS1	16p13.3	0.817	7.98E-91	1.60E-86
LCMT1	16p12.1	0.711	1.16E-58	1.16E-54
PCSK6	15q26.3	-0.669	8.60E-50	5.76E-46
ALDOA	16p11.2	0.648	8.80E-46	4.42E-42
PPIH	1p34.2	0.629	1.83E-42	7.33E-39
METTL9	16p12.2	0.627	3.36E-42	1.12E-38
CLIC1	6p21.33	0.617	1.51E-40	4.35E-37
PKMYT1	16p13.3	0.613	8.77E-40	2.20E-36
TBC1D10B	16p11.2	0.611	1.46E-39	3.27E-36
DCTN5	16p12.2	0.608	5.36E-39	1.08E-35
CD2BP2	16p11.2	0.605	1.38E-38	2.51E-35
CCDC189	16p11.2	0.601	5.25E-38	8.79E-35
CAT	11p13	-0.601	6.39E-38	9.87E-35
PIK3R1	5q13.1	-0.599	1.01E-37	1.46E-34
THOC6	16p13.3	0.599	1.18E-37	1.58E-34
PSMC3IP	17q21.2	0.598	1.54E-37	1.93E-34
TUBA1B	12q13.12	0.596	2.80E-37	3.31E-34
FMO4	1q24.3	-0.594	5.29E-37	5.90E-34
TEDC2	16p13.3	0.592	1.29E-36	1.37E-33
G6PD	Xq28	0.589	3.87E-36	3.89E-33
DMGDH	5q14.1	-0.587	6.62E-36	6.33E-33
BOLA2	16p11.2	0.586	1.04E-35	9.48E-33
RPUSD1	16p13.3	0.584	1.91E-35	1.67E-32
SLC6A1	3p25.3	-0.583	2.42E-35	2.03E-32
FKBP1A	20p13	0.581	5.33E-35	4.28E-32
ALDH5A1	6p22.3	-0.579	9.30E-35	7.18E-32
SNRPA	19q13.2	0.578	1.13E-34	8.39E-32
NUDT1	7p22.3	0.578	1.39E-34	9.98E-32
VASP	19q13.32	0.577	1.47E-34	1.02E-31
ABCA6	17q24.2-q24.3	-0.577	1.63E-34	1.09E-31
KIF2C	1p34.1	0.575	2.92E-34	1.89E-31
RALY	20q11.22	0.575	3.20E-34	2.01E-31
GLYATL1	11q12.1	-0.574	4.99E-34	3.04E-31
POLR3K	16p13.3	0.573	6.28E-34	3.71E-31
CEP89	19q13.11	0.572	8.84E-34	5.07E-31
APOB	2p24.1	-0.571	1.29E-33	7.22E-31
ZNF213	16p13.3	0.571	1.34E-33	7.28E-31
GPLD1	6p22.3	-0.57	1.70E-33	9.00E-31
SLC2A2	3q26.2	-0.569	1.96E-33	1.01E-30
JPT1	17q25.1	0.569	2.01E-33	1.01E-30
PI4K2B	4p15.2	-0.569	2.50E-33	1.20E-30
MAPRE1	20q11.21	0.569	2.56E-33	1.20E-30
SNRPD1	18q11.2	0.569	2.58E-33	1.20E-30
SEPSECS	4p15.2	-0.568	2.90E-33	1.30E-30
RCC2	1p36.13	0.568	2.95E-33	1.30E-30
MIA2	14q21.1	-0.568	2.98E-33	1.30E-30
FUS	16p11.2	0.567	3.94E-33	1.67E-30
KHDRBS1	1p35.2	0.567	4.07E-33	1.67E-30
CORO7	16p13.3	0.567	4.07E-33	1.67E-30

CYP4A22	1p33	-0.567	4.57E-33	1.84E-30
TLCD4	1p21.3	-0.566	4.89E-33	1.93E-30
UPB1	22q11.23	-0.565	7.68E-33	2.97E-30
RORA	15q22.2	-0.565	8.07E-33	3.06E-30
TACC3	4p16.3	0.565	8.64E-33	3.21E-30
EHHADH	3q27.2	-0.565	8.80E-33	3.21E-30
SLC10A1	14q24.1	-0.564	9.17E-33	3.29E-30
ORC6	16q11.2	0.564	1.11E-32	3.90E-30
MPDZ	9p23	-0.563	1.63E-32	5.63E-30
CDC20	1p34.2	0.562	2.17E-32	7.38E-30
GIT1	17q11.2	0.561	2.89E-32	9.69E-30
RPS2	16p13.3	0.56	3.53E-32	1.16E-29
TMSB10	2p11.2	0.56	3.57E-32	1.16E-29
ACD	16q22.1	0.56	4.02E-32	1.28E-29
RMDN2	2p22.2	-0.559	5.47E-32	1.72E-29
DNASE1	16p13.3	0.557	9.17E-32	2.83E-29
PHF19	9q33.2	0.556	1.14E-31	3.48E-29
SLC9B2	4q24	-0.556	1.16E-31	3.49E-29
METTL7A	12q13.12	-0.556	1.19E-31	3.51E-29
KNOP1	16p12.3	0.556	1.30E-31	3.80E-29
EME1	17q21.33	0.555	1.44E-31	4.14E-29
CERS5	12q13.12	0.555	1.50E-31	4.24E-29
LUC7L	16p13.3	0.554	2.05E-31	5.73E-29
STX4	16p11.2	0.553	3.37E-31	9.27E-29
AXIN1	16p13.3	0.552	3.98E-31	1.08E-28
SNRPD2	19q13.32	0.552	4.18E-31	1.12E-28
PCK2	14q11.2-q12	-0.551	4.88E-31	1.29E-28
SC5D	11q23.3-q24.1	-0.55	6.98E-31	1.82E-28
DAZAP1	19p13.3	0.55	7.83E-31	2.02E-28
MTFR2	6q23.3	0.549	9.86E-31	2.49E-28
SFPQ	1p34.3	0.549	9.93E-31	2.49E-28
GYS2	12p12.1	-0.549	1.04E-30	2.59E-28
FMO3	1q24.3	-0.549	1.06E-30	2.60E-28
COL18A1	21q22.3	-0.548	1.12E-30	2.70E-28
PGP	16p13.3	0.548	1.17E-30	2.79E-28
IFI27L2	14q32.12	0.548	1.43E-30	3.39E-28
H2AFZ	4q23	0.547	1.64E-30	3.82E-28
HSD17B4	5q23.1	-0.547	1.84E-30	4.26E-28
HSD17B6	12q13.3	-0.547	1.91E-30	4.36E-28
MYO1B	2q32.3	-0.546	2.36E-30	5.30E-28
PKM	15q23	0.546	2.37E-30	5.30E-28
MFSD10	4p16.3	0.545	2.92E-30	6.45E-28
BIRC5	17q25.3	0.545	3.40E-30	7.43E-28
H2AFX	11q23.3	0.544	3.57E-30	7.70E-28
ZNF580	19q13.42	0.544	3.73E-30	7.97E-28
GATM	15q21.1	-0.544	4.63E-30	9.79E-28
IQGAP2	5q13.3	-0.543	5.57E-30	1.16E-27
RMI2	16p13.13	0.543	6.21E-30	1.29E-27
NAP1L1	12q21.2	0.542	7.78E-30	1.60E-27
MAT1A	10q22.3	-0.542	8.18E-30	1.66E-27
CCNF	16p13.3	0.541	9.42E-30	1.89E-27

Table S2. Differentially-expressed genes of HCCM cell

DHRS2
PCDH1
GANAB
CYP2S1
PCNX3
ABLIM3
SUMO3
IGFL2-AS1
PIP5K1A
HSP90AA1
MT2A
ETV4
COL16A1
KRT80
ITPR1
TSPAN14
SERPINE2
NIPA1
TGFBI
C9orf3
NUFIP2
SMG1
DSP
SERPINH1
BTBD3
MT1E
DACT1
USP9X
SPINK6
SLC38A1
EPRS
TUBA1A
USP34
FAM208B
ADAM15
EIF3A
NEURL1B
CHD9
DYNLT1
EMP1
TPM4
TEAD1
GPRC5A
ATP6V1A
CSNK1G1
PEA15
ITGA3
KDELC2
MACF1
EIF5B
IER3
AKR1B1
MGAT4B
SRSF11
IQGAP1
DIO2
LUC7L3
ATP11C
P3H2
ZC3H13
PNN
SLC7A11
MKI67
FAM78A
BCL2L1
DCLK1
DICER1
VOPP1
AMTN
FTH1
MALAT1
PLXND1
MKNK2
AHCTF1
TAF1
PDE4D
NT5E
SUN2
H19
STC2
THOC2
QSER1
CLSTN1
PDE2A
TAF2
ZMYM4
SREBF2
MT-TN
TTC37
ANKRD17
CALM3
CKAP5
LIFR
SERPINE1
C6orf62
TOPBP1
LPP
CD82

WNK1
ATP13A3
DMXL2
DDX21
FN1
TMEM131
NKTR
TMEM158
TULP4
MYOCD
ACO2
ADI1
MT-RNR1
PDCD6IP
TNKS2
BIRC7
ZNF195
ZDHHC16
PDE3A
OPA1
CCAR1
MYCBP2
TMEM43
TBL1XR1
CASC19
ARHGAP21
IFIT2
ZFR
MGA
PLA2G15
ELFN2
POGZ
LYSMD3
SDAD1
MT-TC
LRRC75A-AS1
PBXIP1
ATR
BAZ1B
RPIA
HECTD1
ZCCHC3
ASH1L
RPL15P3
PRRC2C
RPS2P46
ULBP2
JMY
POU3F2
LNPEP
AKR1C3
SPINK5
PHC3
FSTL4
SEMA3B
COL7A1
PIK3CB
ITGB4
CMTM3
RNF182
PIK3C2A
THSD4
TANC2
LRPPRC
ATAD2
CEP295
KTN1

Table S4. Differentially-expressed genes of intersected

ABLIM3
ADAM15
AKR1C3
ARHGAP21
CASC19
CSNK1G1
ETV4
GANAB
IER3
IQGAP1
KDELC2
MKNK2
NEURL1B
PCNX3
PDE4D
PLXND1
RPIA
SERPINE1
SERPINH1
SLC38A1
SLC7A11
TGFBI
TPM4
TULP4
UBE2I
ZCCHC3
ZDHHC16